Journal of Solution Chemistry (2018) 47:993–1020
https://doi.org/10.1007/s10953-018-0772-6

Behavior of Ionic Liquids Around Charged Metal Complexes: Investigation of Homogeneous Electron Transfer Reactions Between Metal Complexes in Ionic Liquids

Takuya Mabe[1] · Fumiaki Doseki[1] · Takeyoshi Yagyu[2] · Koji Ishihara[3] · Masahiko Inamo[4] · Hideo D. Takagi[1]

Received: 3 September 2017 / Accepted: 11 February 2018 / Published online: 21 June 2018

Abstract

The second-order electron transfer reaction between the photo-excited triplet state of [Zn(TPP)]* (TPP = 5,10,15,20-tetraphenylporphyrin) and $[Co(sep)]^{3+}$ (sep = sepulchrate = 1,3,6,8,10,13,16,19-octaazabicyclo[6.6.6]eicosane) was investigated in three ionic liquids (ILs, 1-R-3-methylimidazolium bis(trifluoromethylsulfonyl)imide with R = butyl, pentyl, and hexyl) and in acetonitrile. Results of electrochemical and kinetic measurements indicated that ILs dissociate in the vicinity of charged metal complexes and at electrodes, although the dissociated anionic and cationic components of the ILs seem to exist as pairs around the metal complexes. Second-order rate constants for the electron transfer reaction are 1.88×10^9, 3.65×10^7, 2.63×10^7, and 2.01×10^7 $kg \cdot mol^{-1} \cdot s^{-1}$ in acetonitrile and in the butyl, pentyl and hexyl ILs, respectively, at 298 K, after correction of the contribution of diffusion. The average slope of the plot of the logarithmic second-order rate constants observed in acetonitrile and ILs against the logarithmic viscosity of each solvent was −0.84. However, the slope of the same plot was much steeper (−4.1) when data for only the three ILs were used. Detailed analyses of the experimental results on the basis of the Latner–Levin cross relation and the Marcus theory lead to the conclusion that the solvent properties such as the dielectric constant and refractive index around the polarized/charged transition states are different from those for the bulk ILs: observed self-exchange rate constants did not exhibit the Pekar factor dependence when dielectric constants and refractive indices for bulk ILs are used.

✉ Masahiko Inamo
minamo@auecc.aichi-edu.ac.jp

✉ Hideo D. Takagi
h.d.takagi@nagoya-u.jp

[1] Research Center for Materials Science, Nagoya University, Nagoya 464-8602, Japan

[2] Department of Life Science and Applied Chemistry, Graduate School of Engineering, Nagoya Institute of Technology, Nagoya, Japan

[3] Department of Chemistry, School of Science and Engineering, Waseda University, Tokyo 169-8555, Japan

[4] Department of Education, Aichi University of Education, Kariya 448-8542, Japan

Keywords Ionic liquid · Electron transfer reaction · Metal complexes

1 Introduction

In a previous study [1], we reported that the slow first-order thermal *Z* to *E* isomerization of azobenzene through the inversion mechanism with a non-polar transition state was hardly influenced by the solvent properties, while the rate constant and the frequency factors of the Arrhenius plots were significantly reduced in ionic liquids for the isomerization of 4-dimethylamino-4′-nitro-azobenzene compared with the reactions in molecular solvents with similar dielectric properties. As this reaction proceeds through the rotation mechanism with a polar transition state, the observed unusually small frequency factors of 10^4–10^7 s^{-1} were attributed to the slow rearrangement of the cationic (1-R-3-methylimidazolium) and anionic (bis(trifluoromethylsulfonyl)amide) components of the ILs to form highly ordered solvation shells around the charge centers of the reactant in the transition state, and such motions of the cationic and anionic components of ILs was accompanied by the concerted movements of the counter ions.

To examine the behavior of ILs around polarized/charged species in more detail, we attempted to examine second-order electron transfer/electron self-exchange reactions of various redox couples in the same ILs, since theories for electron transfer reactions have been well-established for analyzing the solvent reorganization during the activation process [2–10]. Second-order electron transfer reactions between metal complexes may also provide further information about the solvent properties from a different view point.

However, in the preliminary attempts it was found that most metal complexes are not stable in ILs: almost all the inert metal complexes even with bidentate/tridentate ligands decomposed rather rapidly in ILs, probably because of the abundant anionic (cationic) components of ILs (such phenomena strongly indicate that ILs dissociate in the vicinity of charged metal complexes). Other factors that prevented us from making such experiments in ILs are related to the methods for investigations: rapid mixing technique such as the stopped-flow method cannot be used because of the large viscosity of ILs and the use of the NMR line broadening technique was limited to the direct observation of metal centers because of many intense signals of the nuclei on ILs. Therefore, reported investigations of homogeneous redox reactions in ILs depend mostly on the EPR method, the laser flash method and pulse radiolysis [8, 11–13]. On the other hand, various heterogeneous reactions in ILs on the surface of modified electrodes have been reported [14–16]. However, the detailed theoretical analyses of the heterogeneous rate constants are hardly possible, since the dimensions of the electrochemical electron transfer rate constant are $cm \cdot s^{-1}$ and direct comparisons with the homogeneous rate constant is almost impossible [3, 4]. Redox couples so far investigated as homogeneous reactions in ILs have been limited to small organic molecules/counter cationic radicals such as TCNE/$TCNE^{+\cdot}$ [9–13, 17, 18]. The electron transfer/self-exchange reactions for small organic molecules are usually very rapid because of the very small activation barriers for the inner-sphere reorganization. For some reactions, electron transfer rate constants involving the photo-excited states were reported to be faster than the estimated diffusion limit in ILs [11–13], although the intrinsic electron transfer rate constants observed in ILs were certainly slower than those observed in molecular solvents [19, 20]. A thorough investigation of the homogeneous electron self-exchange reaction of the TCNE/$TCNE^{+\cdot}$ couple in various ILs was reported by Grampp and co-workers, and

their detailed analyses revealed that the observed self-exchange rate constants did not exhibit the Pekar factor dependence when the refractive indices and dielectric constants for bulk ILs were employed for the analyses [17].

In this study, we found the $[Zn(TPP)]^{+\cdot/0}$ couple and the caged $[Co(sep)]^{3+/2+}$ couple [21] (TPP = 5,10,15,20-tetraphenyl porphyrin and sep = sepulchrate = 1,3,6,8,10,13,16,19-octaazabicyclo[6.6.6]eicosane) are indefinitely stable in most ILs, and investigated the redox reaction between the triplet excited state of [Zn(TPP)], $[Zn(TPP)]^{*}$, and $[Co(sep)]^{3+}$ and the back electron transfer reaction from $[Co(sep)]^{2+}$ to the π-cation radical $[Zn(TPP)]^{+\cdot}$ using the laser flash technique. The contribution of the viscosity of ILs to the rate constants was isolated using the Kramers theory, and the contribution of the outer-sphere reorganization energy to the total activation Gibbs (free) energy for the self-exchange processes of $[Co(sep)]^{3+/2+}$ and $[Zn(TPP)]^{+\cdot/*}$ couples was estimated on the basis of the Ratner–Levin cross relation for the cross reactions [21–23] and of the Marcus–Sutin model for the self-exchange reactions [2]. The differences between the experimentally isolated and theoretically calculated outer-sphere contributions to the activation Gibbs energies are compared and discussed in relation to the modification of the solvent structures and solvent properties around the charged encounter complexes.

2 Experimental Section

2.1 General

1-Chlorobutane (> 98.0%), 1-chloropentane (> 99.0%), and 1-chlorohexane (> 95.0%) were obtained from Tokyo Kasei (EP grade) and used without further purification. 1-Methylimidazole (Tokyo Kasei EP grade, > 99.0%) was distilled under reduced pressure before use. Activated charcoal and active alumina was obtained from Nakarai and Merck, respectively. Lithium bis(trifluoromethanesulfonyl)imide ($LiNTf_2$) from Fluorochem (99%) was dried at 80–120 °C for 19 h before use.

Acetonitrile obtained from Wako Pure Chemicals Inc. (99.5%) was treated with dried molecular sieves 4A for several days followed by distillation under an argon atmosphere. This treatment reduced the content of water to less than 1 $mmol \cdot kg^{-1}$ [24]. Tetrabutylammonium tetrafluoroborate ($TBABF_4$) from Tokyo Kasei (> 98.0%) and tetrabutylammonium perchlorate (TBAP) from Wako (> 98.0%) were recrystallized twice from ethyl acetate (99.5%)–hexane (96%) mixtures and dried under reduced pressure. All reagents and solutions were handled under an argon atmosphere.

2.2 Syntheses

All ionic liquids, 1-R-3-methylimidazolium chloride 1-R-3-methylimidazolium bis(trifluoromethanesulfonyl)imide (R = butyl, pentyl, and hexyl) were synthesized by the reported method [1, 25, 26] and dried in a vacuum oven at 60 °C for 48 h. The purity of the synthesized ILs were satisfactory as determined by the NMR analyses and the amount of water in the ionic liquids was less than 5 $mmol \cdot kg^{-1}$ for all of the ionic liquids used in this study [1].

2.2.1 $BMIMNTf_2$

^{1}H-NMR(chloroform-d_1): $\delta = 8.74$ ppm (s, 1H; NCHN), 7.32 ppm (m, 2H; NCHCHN), 4.17 ppm (t, $J = 7.6$ Hz, 2H;NCH_2), 3.94 ppm (s, 3H; CH_3N), 1.85 ppm (q, $J = 7.5$ Hz, 2H; NCH_2CH_2), 1.36 ppm (sext, $J = 7.4$ Hz, 2H; $N(CH_2)_2CH_2$), 0.96 ppm (t, $J = 7.6$ Hz, 3H;CH_3CH_2). Elemental analysis calcd. (%) for $C_{10}H_{15}N_3O_4S_2F_6$: C 28.64, N 10.02, H 3.61; found: C 28.63, N 9.72, H 3.65.

2.2.2 $PMIMNTf_2$

^{1}H-NMR (chloroform-d_1): $\delta = 8.76$ ppm (s, 1H; NCHN), 7.29 ppm (m, 2H; NCHCHN), 4.16 ppm (t, $J = 7.6$ Hz, 2H; NCH_2), 3.94 ppm (s, 3H; CH_3N), 1.87 ppm (q, $J = 7.6$ Hz, 2H; NCH_2CH_2), 1.34 ppm (m, 4H; $CH_3(CH_2)_2$), 0.90 ppm (t, $J = 6.8$ Hz, 3H; CH_3CH_2). Elemental analysis calcd. (%) for $C_{11}H_{17}N_3O_4S_2F_6$: C 30.49, N 9.70, H 3.95; found: C 30.45, N 9.38, H 3.99.

2.2.3 $HMIMNTf_2$

^{1}H-NMR (chloroform-d_1): $\delta = 8.79$ pm (s, 1H; NCHN), 7.29 ppm (m, 2H; NCHCHN), 4.17 ppm (t, $J = 7.6$ Hz, 2H; NCH_2), 3.95 ppm (s, 3H; CH_3N), 1.86 ppm (q, $J = 7.3$ Hz, 2H; NCH_2CH_2), 1.33 ppm (m, 6H; $CH_3(CH_2)_3$), 0.88 ppm (t, $J = 7.0$ Hz, 3H; CH_3CH_2). Eelemental analysis calcd. (%) for $C_{12}H_{19}N_3O_4S_2F_6$: C 32.21, N 9.39, H 4.28; found: C 32.41, N 9.18, H 4.39.

2.2.4 $[Co(sep)](NTf_2)_3$

$[Co(sep)]Cl_3$ (Strem, 95%) was recrystallized from water and treated with $AgNTf_2$ (> 98%). White precipitates of AgCl were filtered using diatomaceous earth (from Wako) and the product crystallized. The orange crystal was recrystallized from water and dried in vacuo. Anal. (calcd.) for C, 17.8 (18.2); H, 2.81 (2.55); N, 13.2 (13.0). It has been known that results of the elemental analyses of the compound containing C–F bonds tend to report lower values for carbon and higher value for nitrogen for metal complexes because of incomplete combustion [27]. Purity of this compound was confirmed also by the UV–VIS absorption spectra [21].

2.3 Measurements

Cyclic voltammograms were recorded using a BAS 100BW. A glassy carbon electrode (1 or 3 mm·ϕ) and a Pt wire (0.5 mm·ϕ) were used as the working electrode and the counter electrode, respectively. A $Ag/AgNO_3$ reference electrode containing 10 mmol·kg^{-1} $AgNO_3$ and 0.1 mol·kg^{-1} TBAP in acetonitrile was used for all measurements. UV–VIS–NIR absorption spectra were recorded using a JASCO V-570 spectrophotometer. A JEOL JNM-400 NMR was used to record the NMR signals. Time-resolved absorption measurements were carried out with a Nd-YAG laser (Minilite, Continuum) equipped with a second (532 nm) harmonic generator. The energy and duration of the laser pulse were 12 mJ per pulse and 3–5 ns, respectively. The transient absorption spectra were measured using a photodiode array detector in the multi-channel spectrophotometer system, and absorbance–time traces

were acquired by a photomultiplier detector with a single-wavelength monochromator system (TSP-1000, Unisoku).

Kinetic data and transient absorption spectra were stored and processed using a Unisoku TSP-1000 spectrometer. Refractive indices of the ionic liquids were measured using an Atago 3850 refractometer (PAL-RT).

3 Results and Discussion

3.1 Redox Potentials for the $[Co(sep)]^{3+/2+}$ and $[Zn(TPP)]^{+\cdot/0}$ Couples in Ionic Liquids

Cyclic voltammograms of $[Co(sep)]^{3+}$ and [Zn(TPP)] were examined in acetonitrile, BMIM, PMIM and HMIM (ionic liquids used in this study are abbreviated as BMIM, PMIM and HMIM for 1-R-3-methylimidazolium bis(trifluoromethylsulfonyl)amide with R = butyl, pentyl, and hexyl, respectively, since the counter anion is common, bis(trifluoromethylsulfonyl)amide, NTf_2^-). Results for the $[Co(sep)]^{3+/2+}$ couples are summarized in Table 1. The redox potential for the ferricinium/ferrocene couple in the same solvent was set to zero volt.

As shown in Table 1 (and also Table 2), the redox potential for the highly charged $[Co(sep)]^{3+/2+}$ couple is very different in acetonitrile and in the ILs, while the redox potential is only 6–11 mV more positive with the added $LiNTf_2$ salt in ILs, compared with the measured value without $LiNTf_2$. Somewhat higher values of E_0 in ILs with $LiNTf_2$ indicate that the double layer structure and the solvation environment in the bulk were altered by the addition of this salt, especially by the presence of Li^+ ion with its high charge density. The effect was largest in acetonitrile: when the TBAP (tetrabutylammonium perchlorate) was replaced by $LiNTf_2$, E_0 for the $[Co(sep)]^{3+/2+}$ couple was shifted by +55 mV. In contrast to this drastic shift of E_0 in acetonitrile, the much smaller shift of E_0 in ILs with the addition of $LiNTf_2$ indicates that significant portions of the positive and negative components that constitute the ILs are ionized (dissociated) in the vicinity of the electrodes and the added small amount of lithium salt did not significantly alter the double layer structure. Israelachvili and co-workers reported that less than 0.1% of ILs are dissociated in the pure ILs while ILs in the double layer are significantly ionized, from the results of surface force measurements with thermodynamic arguments [28]. In addition, the voltammogram of the $[Zn(TPP)]^{+\cdot/0}$ couple is reversible under the experimental conditions described later in this section. Therefore, the electrochemical electron transfer rate constant is much larger for this couple than that for the $[Co(sep)]^{3+/2+}$ couple (the signals for the $[Co(sep)]^{3+/2+}$ couple are quasi-reversible and the peak to peak separation increased with increasing scan rate): the rate constant for the homogeneous electron self-exchange reaction for the $[Co(sep)]^{3+/2+}$ couple is only 5.1 $kg{\cdot}mol^{-1}{\cdot}s^{-1}$, while that for the $[Zn(TPP)]^{+\cdot/0}$ couple was estimated as 8.39×10^9 $kg{\cdot}mol^{-1}{\cdot}s^{-1}$ in acetonitrile from the result of this study (see Table 4 below). It is also known that the heterogeneous electron exchange reaction at electrodes is a mirror image of the corresponding homogeneous self-exchange reaction: $\Delta G^*_{\text{heterogeneous}} = \frac{\Delta G^*_{\text{homogeneous}}}{2}$ [3, 4], which indicates that the solvation environment around the metal complexes is identical to that in the vicinity of the electrodes, including the diffuse double layer, where electron transfer reactions take place. Therefore, ILs in the vicinity of charged metal complexes may also be dissociated: cationic components of solvent ILs besiege

Table 1 Results of electrochemical measurements for the $[Co(sep)]^{2+/3+}$ couple

	Supporting electrolyte	E^o ($[Co(sep)]^{2+/3+}$) versus $E^o(Fc^{0/+})$ (mV)	Scan rate v $(mV{\cdot}s)^{-1}$	E_p (anodic) versus $E^o(Fc^{0/+})$ (mV)	i_p (anodic) (μA)	$E_p$cathodic) versus $E^o(Fc^{0/+})$ (mV)	i_p (cathodic) (μA)	Peak separation ΔE^{p-p} (mV)
AN	TBAP[a]	−736[d]	100	−702	1.08	−770	−1.88	68
AN	$LiNTf_2$[b]	−681[d]	100	−635	1.21	−727	−1.83	93
BMIM	–[c]	−586[d]	20	−542	9.67×10^{-2}	−630	−0.114	88
BMIM	$LiNTf_2$[b]	−580[d]	20	−515	9.79×10^{-2}	−645	−0.102	130
PMIM	–[c]	−593[e]	20	−551	8.53×10^{-2}	−634	-9.60×10^{-2}	83
PMIM	$LiNTf_2$[b]	−580[d]	20	−523	8.75×10^{-2}	−638	−0.104	115
HMIM	–[c]	−596[d]	20	−556	8.73×10^{-2}	−637	-9.84×10^{-2}	82
HMIM	$LiNTf_2$[b]	−585[f]	20	−529	9.98×10^{-2}	−640	−0.110	112
AN	TBAP[a]	−733[d]	20	−696	0.278	−770	−0.890	74
AN	$LiNTf_2$[b]	−679[d]	20	−636	0.385	−722	−0.845	86
BMIM	–[c]	−591[d]	100	−532	0.265	−649	−0.287	117
BMIM	$LiNTf_2$[b]	−598[d]	100	−492	0.256	−705	−0.273	213
PMIM	–[c]	−601[e]	100	−551	0.208	−651	−0.225	100
PMIM	$LiNTf_2$[b]	−581[d]	100	−514	0.275	−648	−0.302	134
HMIM	–[c]	−598[d]	100	−550	0.238	−646	−0.266	96
HMIM	$LiNTf_2$[b]	−596[f]	100	−507	0.258	−684	−0.297	177

Concentration of the added supporting electrolyte: [a]0.1 $mol{\cdot}kg^{-1}$ (TBAP), [b]0.1 $mol{\cdot}kg^{-1}$ ($LiNTf_2$), [c]no supporting electrolyte was added

Concentration of metal complex: [d]$[Co(sep)(NTf_2)_3]=1.00$ $mmol{\cdot}kg^{-1}$, [e]$[Co(sep)(NTf_2)_3]=0.99$ $mmol{\cdot}kg^{-1}$, [f]$[Co(sep)(NTf_2)_3]=1.20$ $mmol{\cdot}kg^{-1}$

Table 2 Observed redox potentials for $[Co(sep)]^{3+/2+}$, $[Zn(TPP)]^{+/0}$, and $[Zn(TPP)]^{*/+}$

	Supporting electrolyte	$E^o([Co(sep)]^{2+/3+})$ versus $E^o(Fc^{0/+})$ (mV)	$E^o([Zn(TPP)]^{0/+})$ versus $E^o(Fc^{0/+})$ (mV)	$E^o([Zn(TPP)]^{*/+})$ versus $E^o(Fc^{+/0})$ (V^k)
AN	TBAP[a]	-736 ± 1[d]	372 ± 2[f]	-1.22
AN	$LiNTf_2$[b]	-681 ± 1[e]	373 ± 4[g]	-1.22
BMIM	–[c]	-586 ± 2[e]	330 ± 3[h]	-1.26
PMIM	–[c]	-593 ± 2[e]	320 ± 3[i]	-1.27
HMIM	–[c]	-596 ± 2[e]	316 ± 3[j]	-1.27

Concentration of the added supporting electrolyte: [a]0.1 mmol·kg^{-1} (TBAP), [b]0.1 mol·kg^{-1} ($LiNTf_2$), [c]no supporting electrolyte was added. Concentrations of metal complex: [d]$[Co(sep)(BPh_4)_3] < 1.0$ mmol·kg^{-1}, [e]$[Co(sep)(NTf_2)_3] = 1.0$ mmol·kg^{-1}, [f]$[Zn(TPP)] = 0.98$ mmol·kg^{-1}, [g]$[Zn(TPP)] < 0.78$ mmol·kg^{-1}, [h]$[Zn(TPP)] < 0.16$ mmol·kg^{-1}, [i]$[Zn(TPP)] = 0.14$ mmol·kg^{-1}, [j]$[Zn(TPP)] = 0.15$ mmol·kg^{-1} ([Zn(TPP)]). The redox potential for the $[Zn(TPP)]^{*/+}$ couple was estimated by subtracting the excitation energy of [Zn(TPP)] (1.59 eV) from the redox potential for the $[Zn(TPP)]^{+/0}$ couple (see text); [k]errors are smaller than 0.004 V

the cationic metal complexes surrounded by the anionic components of the ILs, while the ILs in the bulk are unaffected. Such a model explains the smooth diffusion of complex ions in ILs.

Separation between the anodic and cathodic peaks for the $[Co(sep)]^{3+/2+}$ couples became wider when supporting electrolyte ($LiNTf_2$) was added to the IL solutions, indicating that the reversibility of the signals was reduced with the presence of excess $LiNTf_2$. As such changes in the signals are not related to the electrochemical electron transfer rate (conditions for measurements, including the scan rate, were not changed), it is certain that the diffusion-controlled condition necessary for the observation of reversible/quasi-reversible CV signals is spoiled by the existence of added salt: it seems the added salt acted chiefly as a 'structure breaker'. In addition, peak currents of the CV signals hardly changed with the addition of supporting electrolyte (see results in BMIM at scan rate = 20 mV·s^{-1} where the concentrations of $[Co(sep)]^{3+}$ are identical): the migration current is not significant in ILs, even without supporting electrolyte (which is similar to the condition for aqueous solutions with > 0.1 mol·dm^{-3} of supporting electrolyte) [29]. This result is also consistent with the observations by Israelachvili and co-workers [28].

At this stage, we may be able to conclude that: (1) solutions of ionic liquids, BMIM, PMIM and HMIM, can be regarded as moderate electrolyte solutions in the vicinity of the electrodes and probably around the charged metal complexes; (2) introduction of Li^+ to these solutions slightly alters the double layer structure at the electrodes; (3) Li^+ ions in ILs also act as a structure breaker because of its very high charge density, since the observed wider peak to peak separation indicates the altered diffusion of ILs by the presence of Li^+; and (4) on the other hand, small concentrations of charged metal complexes (< 1 mmol·kg^{-1}), $[Co(sep)]^{3+/2+}$ and $[Zn(TPP)]^{+\cdot}$, did not alter the double layer structure as well as the solvent structure.

Summarized in Tables 1 and 2 are the redox potentials for $[Co(sep)]^{3+/2+}$ and $[Zn(TPP)]^{+\cdot/0}$ couples measured in acetonitrile and in ILs without supporting electrolyte. The redox potential between the triplet excited state and the π-cation radical $[Zn(TPP)]^+$ was obtained by subtracting $E^o([Zn(TPP)]^{+\cdot/0})$ value (= potential difference between the ground state and π-cation radical) from the energy of the triplet excited state (1.59 eV;

a phosphorescence maximum was observed at ca. 778 nm) which is 0.47 eV lower in energy than the singlet excited state (2.06 eV; fluorescence maximum 601 nm): it is known that fluorescence and phosphorescence maxima are largely independent of the solvent [30–35].

Differences in the observed redox potentials in two different solvents may roughly be dependent on the solvation energies in the two solvents and therefore it is given by the following equations: Eq. 1 corresponds to the classical Born-type equation, and Eq. 2 to the MSA (Mean Spherical Approximation) equation with the radius of the solvent being a_0 [6, 36–40].

$$F\left(E_a - E_b\right) = -\frac{N_A e^2}{8\pi\varepsilon_0}\left(\frac{(n-1)^2}{r_B} - \frac{n^2}{r_A}\right)\left(\frac{1}{\varepsilon_a} - \frac{1}{\varepsilon_b}\right) \tag{1}$$

$$F\left(E_a - E_b\right) = -\frac{N_A e^2}{8\pi\varepsilon_0}\left(\frac{z_B^2}{r_B} - \frac{z_A^2}{r_A}\right)\left[\left(1 - \frac{1}{\varepsilon_b}\right)\frac{1}{1+\delta_2(\varpi=0)} - \left(1 - \frac{1}{\varepsilon_a}\right)\frac{1}{1+\delta_1(\varpi=0)}\right] \tag{2}$$

where $\delta = \frac{3a_0}{r[108^{\frac{1}{3}}\varepsilon^{\frac{1}{6}} - 2 < Para >]}$.

When the ionic radii of both $[Co(sep)]^{3+}$ and $[Co(sep)]^{2+}$ are set to r (this assumption is valid since $[Co(sep)]^{3+}$ and $[Co(sep)]^{2+}$ are caged metal species) [41], these equations are given by

$$F\left(E_a - E_b\right) = \Delta G_b^{solv} - \Delta G_a^{solv} = -\frac{N_A e^2}{8\pi\varepsilon_0}\left(\frac{(n-1)^2 - n^2}{r}\right)\left(\frac{1}{\varepsilon_a} - \frac{1}{\varepsilon_b}\right) \tag{1'}$$

$$F\left(E_a - E_b\right) = -\frac{N_A e^2}{8\pi\varepsilon_0}\left(\frac{(n-1)^2 - n^2}{r}\right)\left(\left(1 - \frac{1}{\varepsilon_b}\right)\frac{1}{1+\delta_2(\varpi=0)} - \left(1 - \frac{1}{\varepsilon_a}\right)\frac{1}{1+\delta_1(\varpi=0)}\right) \tag{2'}$$

where ε is the relative dielectric constant and the subscript a and b refer to the two different solvents, and z_1, and z_2 are the formal charges of the metal complexes, respectively. By comparing the measured redox potentials for the $[Co(sep)]^{3+/2+}$ couple in ILs and the redox potential measured in acetonitrile, apparent values of the relative dielectric constant for each IL were calculated. The estimated value of the apparent dielectric constant by the Born-type equation is ca. 26 for all ILs. Estimated radii of ILs by the MSA equation (Eq. 2′) are a_0=222 pm when ε is 17.5 [1] (a_0=265 pm when ε is 26). Values of a_0 are small (a_0=195 pm) for PMIM (ε=13.0), and a_0=186 pm for HMIM (ε=12.7) [42, 43]. Although it is known that MSA estimates rather small values for a_0 [6], these values estimated by Eq. 2′ may indicate that ILs in the vicinity of charged solutes behaves as the dissociated component ions.

On the other hand, the CV signals are reversible for the $[Zn(TPP)]^{+/0}$ couple, indicating that electron transfer at the electrode is very rapid. The wider peak to peak separation observed for the $[Co(sep)]^{3+/2+}$ couple, under the same experimental conditions, indicates that the electron transfer process is slower for the $[Co(sep)]^{3+/2+}$ couple; it is known that the self-exchange rate constant for the $[Co(sep)]^{3+/2+}$ couple is much smaller than that for the $[Zn(TPP)]^{+/0}$ couple [42]. The redox potential for the $[Zn(TPP)]^{+/0}$ couple was not altered by the addition of supporting electrolyte, $LiNTf_2$. It seems that the double layer structure was not altered by addition of $LiNTf_2$, since the redox potential is at the positive side. The solvent environment around this redox pair seems not to be affected significantly

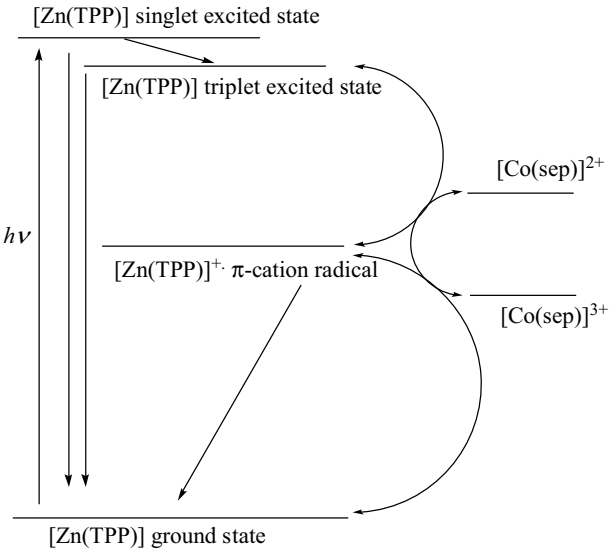

Scheme 1 Scheme of the overall photo reaction examined in this study

because of the very low charge density of $[Zn(TPP)]^{+\cdot}$ species. Application of Eqs. 1 and 2 to the results for the $[Zn(TPP)]^{+\cdot/0}$ couple was not successful with the same reasons. It seems that the low charge density with long conjugate system of $[Zn(TPP)]^{+\cdot}$ does not induce significant dissociation of the surrounding ILs.

As the addition of supporting electrolytes to ILs significantly modified the solvent properties, kinetic experiments were carried out without using a supporting electrolyte.

3.2 Flash Photolysis Experiments

The Marcus–Sutin theory [2] predicts contributions of inner- and outer-sphere reorganization energies for the self-exchange process, and the rate constant k_{ex} is given by Eq. 3.

$$k_{ex} = K_{OS}\kappa_{el}\nu_n\kappa_n \tag{3}$$

where κ_{el}, ν_n, and κ_n are the electronic transmission coefficient, the nuclear vibrational frequency given generally by k_BT/h, and the nuclear factor given by $\exp(-\Delta G^*/RT)$, respectively [2]. ΔG^* includes the sum of the inner- and outer-sphere contributions to the activation Gibbs energy in the case of electron self-exchange reaction: when the energy to form the encountered complex (precursor complex) is included, ΔG^* includes $\Delta G^*_{Fuoss} = -RT\ln K_{OS}$.

The reactions of photo-activated $[Zn(TPP)]^0$ in molecular solvents have been well established [44–47] and the photo-processes are shown in Scheme 1. It is known that the lifetime of the singlet photo-excitation product of [Zn(TPP)] is ca. 3 ns [33] and it rapidly relaxes to the triplet state by the inter-system crossing. The triplet state [Zn(TPP)]* readily reacts with the oxidizing reagents (metal complexes such as $[Co(sep)]^{3+}$) to form a π-cation radical, $[Zn(TPP)]^{+\cdot}$, followed by the back reaction with reducing reagents (such as $[Co(sep)]^{2+}$) to the ground state $[Zn(TPP)]^0$.

The lifetime of the triplet excited state is long (44 μs in toluene and 230 μs in methanol) [48] and the relatively slow electron transfer to $[Co(sep)]^{3+}$ is expected to be observed by monitoring the decrease in the absorption in the ca. 460 nm region that corresponds to

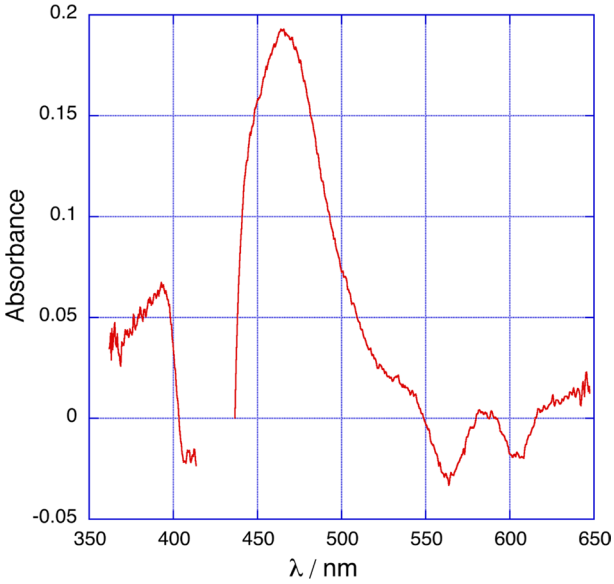

Fig. 1 Typical transient absorption spectrum observed in the range of 350–650 nm in BMIM, after 1 μs of laser irradiation. $[Zn(TPP)] = 9.2 \times 10^{-6}$ mol·kg^{-1}, $[Co(sep)^{3+}] = 4.0 \times 10^{-4}$ mol·kg^{-1}, and $T = 298$ K. Differential spectrum in the rgion from 415 to 430 nm was unreliable and therefore deleted because of the very strong Soret band

the absorption maximum of the triplet excited state or by monitoring the increase in the absorption at 405 nm region for the absorption maximum of the π-cation radical. The overall reaction is described as follows:

$$[Zn(TPP)] \xrightarrow{h\nu} [Zn(TPP)]^*(\text{singlet})$$

$$[Zn(TPP)]^*(\text{singlet}) \rightarrow [Zn(TPP)]^*(\text{triplet})\ \text{intersystem crossing}\ (\sim 3\ \text{ns})$$

$$[Zn(TPP)]^*(\text{triplet}) + \left[Co(sep)\right]^{3+} \xrightarrow{k_1} [Zn(TPP)]^{+\bullet}(\pi\text{-radical}) + \left[Co(sep)\right]^{2+} \quad (4)$$

$$[Zn(TPP)]^{+\cdot}(\pi\text{-radical}) + \left[Co(sep)\right]^{2+} \xrightarrow{k_2} [Zn(TPP)] + \left[Co(sep)\right]^{3+} \quad (5)$$

Typical transient absorption spectra observed in the range of 350–650 nm region are shown in Figs. 1 and 2, both of which were observed at 1 and 250 μs after 532 nm pulse of 5 ns duration. The triplet excited state $[Zn(TPP)]^*$ was observed after 1 μs of the flash at ca. 460 nm in Fig. 1, which decreased by the slow reaction with $[Co(sep)]^{3+}$. As the reaction of the triplet excited state with $[Co(sep)]^{3+}$ produces the π-cation radical, $[Zn(TPP)]^{+\cdot}$, the absorption at ca 405 nm region increased after 250 μs.

Typical kinetic traces observed at 405 and 460 nm are shown in Figs. 3 and 4. The kinetic trace at 460 nm shows that the triplet excited state of [Zn(TPP)]* immediately produced after irradiation was consumed by the reaction with $[Co(sep)]^{3+}$. The kinetic trace observed at 405 nm clearly shows the increase of the absorption by $[Zn(TPP)]^{+\cdot}$ at short times, followed by the decrease of the absorption due to the reaction with $[Co(sep)]^{2+}$. The increase in the absorption at short times corresponds to the creation of the π-cation radical by the reaction of the triplet state with $[Co(sep)]^{3+}$, while it is consumed somewhat more slowly by the reaction with $[Co(sep)]^{2+}$. The concentration of $[Co(sep)]^{3+}$ is sufficiently greater than that of [Zn(TPP)], indicating that the pseudo-first-order conditions can be applied to the analysis. All observed kinetic traces were analyzed by double-exponential functions to isolate rate constants for the two consecutive processes and/or to isolate

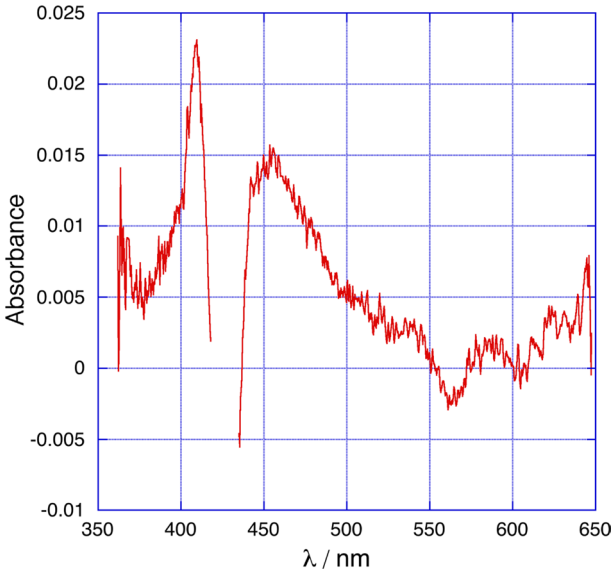

Fig. 2 Typical transient absorption spectrum observed in the range of 350–650 nm in BMIM, after 250 μs of laser irradiation. $[Zn(TPP)] = 9.2 \times 10^{-6}$ mol·kg^{-1}, $[Co(sep)^{3+}] = 4.0 \times 10^{-4}$ mol·kg^{-1}, and $T = 298$ K. Differential spectrum in the region from 415 to 430 nm was unreliable and therefore deleted because of the very strong Soret band

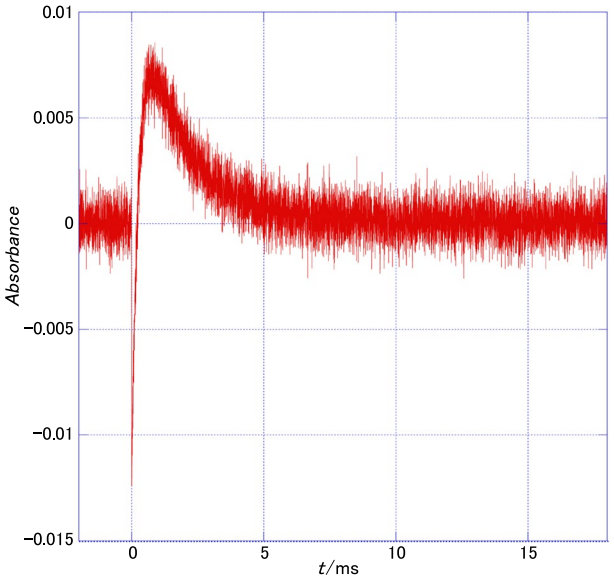

Fig. 3 Typical kinetic trace observed at $\lambda = 405$ nm in BMIM at 298 K. $[Zn(TPP)] = 4.3 \times 10^{-6}$ mol·kg^{-1}, $[Co(sep)^{3+}] = 1.0 \times 10^{-4}$ mol·kg^{-1}

the natural deactivation process of the π-cation radical (see footnote 1). Some of the data in BMIM were[1] analyzed by combining two data sets observed at 405 and 460 nm, and the rate constants were examined to check the consistency with the independent analyses

[1] These reaction curves can be attributed to consecutive reactions:
$A_1 \rightarrow A_2 \rightarrow A_3$.
The absorbance of the reacting solution, A, can be expressed as
$A = P\exp(-k_1 t) + Q\exp(-k_2 t) + R$, where the terms P, Q, and R are functions of the rate constants (k_1 and k_2), molar absorption coefficients of each species, and the initial concentrations of A_1 and A_2. This expression is well documented in many textbooks for chemical kinetics such as [49].

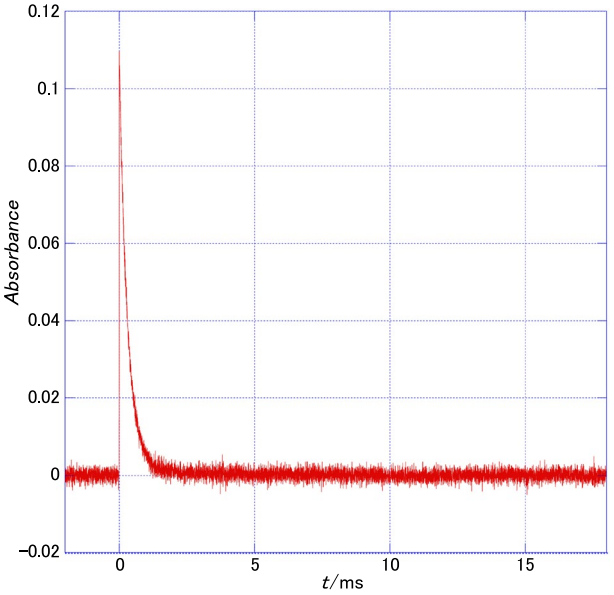

Fig. 4 Typical kinetic trace observed at $\lambda = 460$ nm in BMIM at 298 K: $[Zn(TPP)] = 4.3 \times 10^{-6}$ mol·kg^{-1}, $[Co(sep)^{3+}] = 1.0 \times 10^{-4}$ mol·kg^{-1}

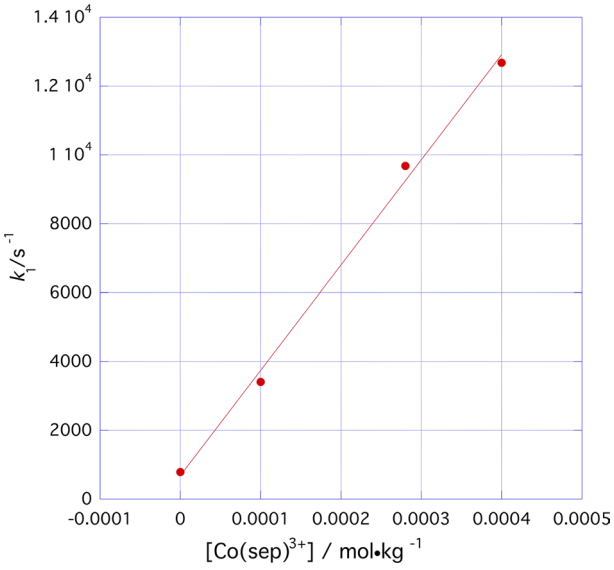

Fig. 5 Dependence of k_1 on $[Co(sep)^{3+}]$ at 298 K in BMIM. $[Zn(TPP)] = 4.3 \times 10^{-6} - 1.30 \times 10^{-5}$ mol·kg^{-1} and $[Zn(TPP)] \ll [Co(sep)^{3+}]$. The slope of the plot corresponds to the second-order rate constant for reaction (4), and the intercept to the decay of the triplet excited state, ^{3}ZnTPP*, via the intersystem crossing to S_0

using data observed at two different wavelengths. In Figs. 5 and 6, the observed first-order rate constants, k_1 and k_2, thus obtained in BMIM are plotted against the concentration of $[Co(sep)]^{3+}$. The rate constant k_1 depends linearly on the concentration of $[Co(sep)]^{3+}$. The

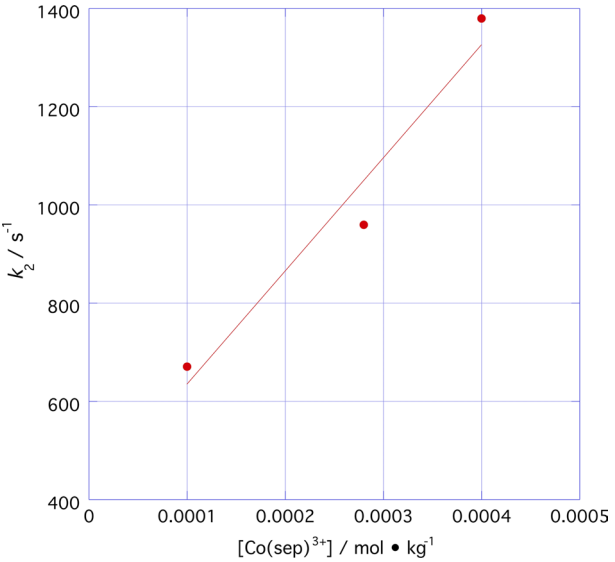

Fig. 6 Dependence of k_2 on the concentration of $[Co(sep)]^{3+}$ at 298 K in BMIM: $[Zn(TPP)] = 4.3 \times 10^{-6} - 1.30 \times 10^{-5}$ mol·kg^{-1} and $[Zn(TPP)] \ll [Co(sep)^{3+}]$

intercept of the linear line of Fig. 5 corresponds to the decay of the triplet excited state of [Zn(TPP)]* to the ground state by intersystem crossing. The second-order rate constant for reaction (4) was obtained from the slope of the plot in Fig. 5. Note that the linear dependence of k_1 on the concentration of $[Co(sep)]^{3+}$ indicates the activity coefficients of ionic species in solutions were hardly changed although the ionic strength of the solution was not adjusted: it seems that charged species such as $[Co(sep)]^{3+}$ are associated with anions in solution and the charge on this species was effectively cancelled.

Time dependence of the absorption change for reaction (5) was expected to be second-order, because the concentration of $[Co(sep)]^{2+}$ is identical to that of π-cation radical. However, the observed rate constants could not be described by a simple second-order reaction: it was close to a first-order process and the plot of this first-order rate constants against the concentration of $[Co(sep)]^{3+}$ is quasi-linear, as shown in Fig. 6, followed by the other first-order reaction. The trace was, as a whole, better described by using a double exponential function.

There are two possibilities to explain the observed kinetic results for reaction (5). One is given by a catalytic reaction involving a trace amount of contaminant, and the other relates to the relative energies of the $[Zn(TPP)]^{+\cdot}$ and $[Co(sep)]^{2+}$energy levels.

3.2.1 Case 1

A small amount of a reactive contaminant, X, catalyzes the reaction as described in reactions (6) and (7).

$$[Zn(TPP)]^{+\cdot} + X \xrightarrow{k_3} [Zn(TPP)] + X^{+} \tag{6}$$

$$X^{+} + \left[Co(sep)\right]^{2+} \xrightarrow{k_4} X + \left[Co(sep)\right]^{3+} \tag{7}$$

Scheme 2 [Zn(TPP)] triplet excited state reduces Co(III) and $[Zn(TPP)]^{+\cdot}$ π-cation radical oxidizes Co(II)

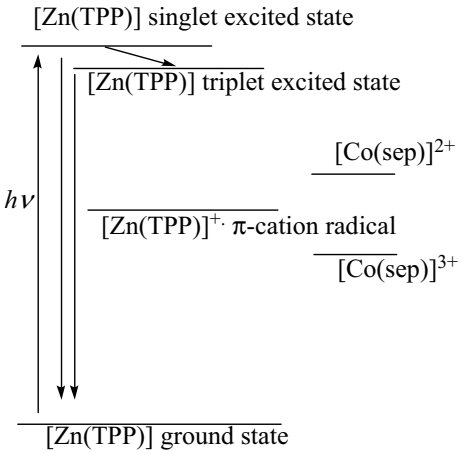

Scheme 3 [Zn(TPP)] triplet excited state reduces Co(III) while $[Zn(TPP)]^{+\cdot}$ π-cation radical cannot oxidize Co(II)

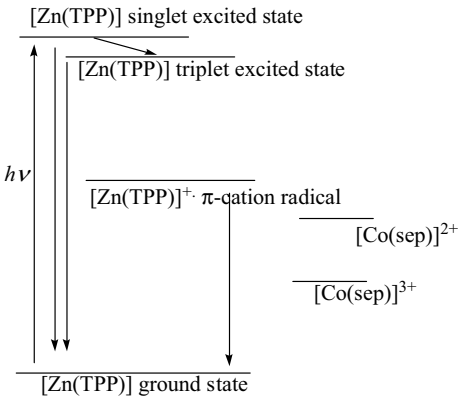

In this case, the kinetic trace of the reaction should be first-order and the observed first-order rate constant may be linearly dependent on the concentration of $[Co(sep)]^{3+}$ when k_4 is large.

3.2.2 Case 2

Another explanation is possible if the π-carion radical $[Zn(TPP)]^{+\cdot}$ produced immediately after the reaction with $[Co(sep)]^{3+}$ is in its excited state: it is possible that the immediate product after reaction (4) is in the structurally excited state since the driving force of reaction (4) is very large. In such a case, there are three possibilities for the deactivation of excited $[Zn(TPP)]^{+\cdot}$: (a) $[Zn(TPP)]^{+\cdot}$ is in its ground state which is lower in energy than $[Co(sep)]^{2+}$ (Scheme 2), (b) $[Zn(TPP)]^{+\cdot}$ is in its ground state which is higher in energy than $[Co(sep)]^{2+}$ (Scheme 3), (c) $[Zn(TPP)]^{+\cdot}$ is in the excited state which is higher in energy than $[Co(sep)]^{2+}$ while it relaxes to its ground state having lower energy than$[Co(sep)]^{2+}$, with a rate constant k (Scheme 4). In the case of (a), a seocnd-order reaction with $[Co(sep)]^{2+}$ should be observed, while in (b) there is no

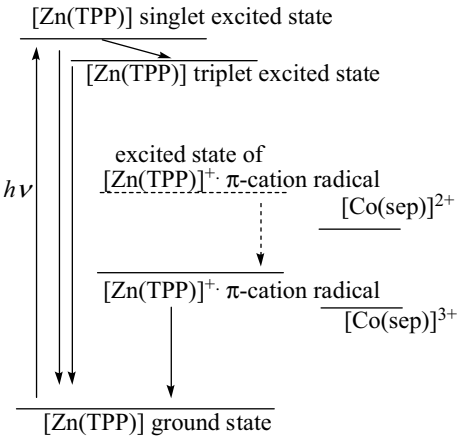

Scheme 4 [Zn(TPP)] triplet excited state reduces Co(III) and an excited state of $[Zn(TPP)]^{+\cdot}$ π-cation radical is formed. However, it cannot oxidize Co(II) unless it relaxes to the ground state of $[Zn(TPP)]^{+\cdot}$ π-cation radical

reaction of $[Zn(TPP)]^{+\cdot}$ with $[Co(sep)]^{2+}$, and we will observe a simple first-order decay of $[Zn(TPP)]^{+\cdot}$ without dependence on $[Co(sep)]^{3+}$. In case (c) as depicted by Scheme 4, the decrease of $[Zn(TPP)]^{+\cdot}$ with time is first-order with the rate constant k when $k << k_2[Co(sep)^{2+}]$. When $k >> k_2[Co(sep)^{2+}]$, we will observe a second-order reaction, while the reaction is expected to be a consecutive process described by a double-exponential function when $k \sim k_2[Co(sep)^{2+}]$.

In Table 3, the second-order rate constants for reaction (4) in three ILs and in acetonitrile are summarized. As it was not possible to obtain accurate second-order rate constants for reaction (5), analyses on the basis of the Marcus theory are carried out essentially for reaction (4) in the following section.

As the second-order rate constants estimated in acetonitrile and ILs are close to the diffusion limits calculated using Eq. 8, it was necessary to isolate the contribution of diffusion from the obtained second-order rate constants. By assuming that the diffusion limit for second-order reactions is given by the Stokes–Einstein equation (Eq. 8) [23], the diffusion limits of the second-order rate constants in acetonitrile and ILs were calculated.

$$k_{\mathrm{diff}} = \frac{2RT\left(r_A + r_B\right)^2}{3000\eta r_A r_B}\left(\frac{U}{\exp(U) - 1}\right), \quad U = \frac{z_A z_B e^2}{4\pi\varepsilon_0\varepsilon\left(r_A + r_B\right)kT} \tag{8}$$

where r_A (=570 pm), r_B (=400 pm), and z_A (=0), z_B (=+3) are the ionic/molecular radii and formal charges of reactants, respectively [50, 52]. The estimated diffusion-controlled rate constants are 1.56×10^{10}, 1.89×10^{8}, 1.68×10^{8}, and 1.56×10^{8} kg·mol^{-1}·s^{-1} (density of each solvent was accounted for) for the reaction between [Zn(TPP)]* and $[Co(sep)]^{3+}$ in acetonitrile, BMIM, PMIM and HMIM, respectively. The rate constants in the last column of Table 3 were calculated using Eq. 9 to remove the contribution of diffusion from the observed second-order rate constants [50–54].

$$\frac{1}{k_{\mathrm{obsd}}} = \frac{1}{k_{\mathrm{diff}}} + \frac{1}{k_{\mathrm{reaction}}} \tag{9}$$

Logarithmic values of the rate constants for reaction (4) thus corrected for the diffusion contribution are plotted against the logarithm of the viscosity of each solvent in Fig. 7. The plot appears to be linear with a slope of −0.834 (average slope, including the rate constant

Table 3 Second-order rate constants for reaction (1) in three IL's and in acetonitrile

	η/cP	η/kg·m^{-1}·s^{-1}	Density, d/kg·dm^{-3}	k_d/kg·mol^{-1}·s^{-1}	Observed k_{12}/kg·mol^{-1}·s^{-1}	Corrected k_{12}/kg·mol^{-1}·s^{-1}
AN	0.339	0.000339	0.777	1.56×10^{10}	$(1.68\pm0.18)\times10^{9}$	$(1.88\pm0.26)\times10^{9}$
BMIM	52	0.052	1.44	1.89×10^{8}	$(3.06\pm0.14)\times10^{7}$	$(3.65\pm0.20)\times10^{7}$
PMIM	57	0.057	1.40	1.68×10^{8}	$(2.27\pm0.06)\times10^{7}$	$(2.63\pm0.08)\times10^{7}$
HMIM	60	0.06	1.37	1.56×10^{8}	$(1.78\pm0.13)\times10^{7}$	$(2.01\pm0.17)\times10^{7}$

Values of k_d and corrected k_{12} were estimated by using Eqs. 10 and 11. [a]$T=298.2\pm1.0$

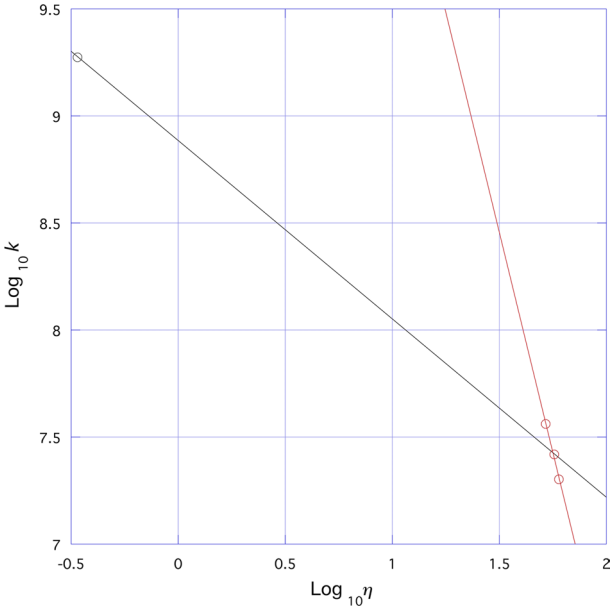

Fig. 7 Plot of logarithmic value of the rate constant k_{12} for cross reactions ($T = 298$ K, and the rate constants were corrected for the diffusion contribution) against the logarithmic value of the apparent (reported) viscosity of solvents (acetonitrile, BMIM, PMIM and HMIM)

observed in acetonitrile) indicating that the dependence of the second order rate constant k_1 on the viscosity of the solvents roughly obeys the predictions of either the Sumi–Marcus theory $\left(\log_{10} k \propto \eta^{-\alpha},\ 0 < \alpha < 1\right)$ [55, 56] or Kramers theory $\left(\log_{10} k \propto \eta^{\alpha},\ \alpha = -1\right)$ [57, 58].

However, the slope of the plot for the data observed in ionic liquids only was much larger (−4.10) as shown by the right three circles in Fig. 7, indicating that the rate constants in ILs are governed by other factors than the macroscopic viscosity.

In the following discussion, the influence of viscosity η was assumed to follow the Kramers theory (=the rate constant depends on η^{-1} through Eqs. 8 and 9, and the effect of the Pekar factor, $\frac{1}{n^2} - \frac{1}{\varepsilon_s}$) (see also Eq. 15 below), on the observed and calculated activation Gibbs energies for the electron self-exchange processes will be discussed.

The Marcus cross relation is generally expressed by Eq. 10 [2], with additional work terms introduced by Espenson [59].

$$k_{AB} = \left(k_{AA} k_{BB} K_{AB} f_{AB}\right)^{1/2} W_{AB},\ \ln f_{AB} = \frac{\left(\ln K_{AB} + \frac{\left(w_{AB} - w_{BA}\right)}{RT}\right)^2}{4 \ln\left(\left(\frac{k_{AA} k_{BB}}{z^2} + w_{AA} + w_{BB}\right)\frac{1}{RT}\right)} \tag{10}$$

where Z is the collision frequency (~10^{12}, which is close to $k_B T/h$ in water and acetonitrile), $W_{AB} = \exp\left(\frac{-\left(w_{AB} + w_{BA} - w_{AA} - w_{BB}\right)}{2RT}\right)$, and w_{ij} is the coulombic work given by $w_{ij} = \frac{z_A z_B e^2}{4\pi\varepsilon\varepsilon_0 r\left(1 + Br\sqrt{\mu}\right)}$: r is the distance between two reactants, μ is the ionic strength and B is a parameter related to the Debye–Huckel theory for electrolyte solutions (μ is unknown for IL solutions). Use of this relation was not successful for the electron transfer reactions involving small hydrated molecules/ions or large molecules/ions such as enzymes [23]. It

was also shown that Eq. 10 does not correctly explain the cross reactions with large K_{AB} values such as the reaction of $[Fe(OH_2)]^{3+}$with $[Co(sep)]^{2+}$ in aqueous acidic solution [60].

In 1980, Ratner and Levin derived a similar cross relation given by Eqs. 11 or 12 solely on the basis of the thermodynamic relations [22, 23]. They used only two assumptions to derive the relation: (a) the activation process for each reactant is independent of the other reactant, and (b) the activated species are the same for the self-exchange and the cross reactions.

$$\Delta G^{*}_{AB} = \frac{1}{2}\left(\Delta G^{*}_{AA} + \Delta G^{*}_{BB} + \Delta G^{0}_{AB}\right) \tag{11}$$

$$k_{AB} = \left(k_{AA}k_{BB}K_{AB}\frac{Z^{2}_{AB}}{Z_{AA}Z_{BB}}\right)^{1/2} \tag{12}$$

where Z's are the collision frequencies for the second-order reaction (given by Eq. 13). Z_{ij} values are ~ 10^{12} for water and ordinary non-viscous fluids and $Z^{2}_{12} \sim Z_{11}Z_{22}$ when the reaction has charge symmetry [23], while the effect of charges on the reactants to Z_{ij} is related to Eq. 8.

$$k_{ij} = Z_{ij}\exp\left(\frac{\Delta G^{*}_{ij}}{RT}\right) \tag{13}$$

Use of the cross relation given by Eqs. 11–13 is more appropriate than the use of Eq. 10 for the analyses of the results obtained in ILs, since it is not possible to correctly estimate the work terms of the reactants (we do not know the ionic strengths of the solutions nor the exact properties of the solvents in the vicinity of solutes necessary for the use of Eq. 10).

However, Eq. 10 is the standard theoretical equation and is reliable for analyses of the reactions in conventional molecular liquids. Therefore, we used Eq. 10 for the estimation of activation parameters of the reactions in acetonitrile. Use of Eqs. 11 and 12 seems the more appropriate for the analyses of the reactions observed in ILs, since the contributions of $\Delta G^{*}_{\text{Fuoss}}$ and the frequency factor of reactions are included in Z_{ij}, and some parameters necessary for the calculations of $\Delta G^{*}_{\text{Fuoss}}$ are unavailable for ILs. The quotient $\frac{Z^{2}_{AB}}{Z_{AA}Z_{BB}}$ was taken to be ca. 1 for the estimation of the kinetic parameters of the reactions in ILs since effective charge cancellation of Co(III)/(II) complexes by counter anions is expected from the small bulk dielectric constants of the solvents used in this study [see Appendix 1 for the justification of this assumption].

The total activation Gibbs energy for a self-exchange reaction in acetonitrile is given by the following equation [2, 23].

$$\Delta G^{*}_{\text{Total}} = \Delta G^{*}_{\text{OS}} + \Delta G^{*}_{\text{IS}} + \Delta G^{*}_{\text{Fuoss}} \tag{14}$$

where ΔG^{*}_{OS}, ΔG^{*}_{IS}, and $\Delta G^{*}_{\text{Fuoss}}$ are the outer-sphere activation Gibbs energy, the inner-sphere activation Gibbs energy and the energy to bring two reactants to form a precursor complex $\left(\Delta G^{*}_{\text{Fuoss}} = -RT\ln K_{\text{OS}}\right)$. ΔG^{*}_{OS} and $\Delta G^{*}_{\text{Fuoss}}$ terms are given by Eqs. 15 and 16 [2–8, 23]:

$$\Delta G^{*}_{\text{os}} = \frac{Ne^{2}}{16\pi\varepsilon_{0}}\left(\frac{1}{\varepsilon_{op}} - \frac{1}{\varepsilon_{s}}\right)\left(\frac{1}{2r_{1}} + \frac{1}{2r_{2}} - \frac{1}{r_{12}}\right) \tag{15}$$

Table 4 Kinetic parameters calculated for the self-exchange reaction of the $[Zn(TPP)]^{+\cdot/*}$ couple in acetonitrile by applying the cross relation to the rate constant for the cross reaction of $[Zn(TPP)]^{*}$ with $[Co(sep)]^{3+}$

k_{11}/kg·mol^{-1}·s^{-1}	ΔG^{*}_{11}/kJ·mol^{-1}[a]	$\Delta G_{\mathrm{Fuoss}}$/kJ·mol^{-1}	$\Delta G^{*}_{\mathrm{OS}}$/kJ·mol^{-1}[b]	$\Delta G^{*}_{\mathrm{IS}}$/kJ·mol^{-1}[c]
8.39×10^{9}	16.4	0	15.5	0.844

[a] $\Delta G^{*}_{11} = -RT\ln(k_{11}h/k_{\mathrm{B}}T)$ was used for the calculation

[b] $r(\mathrm{Zn}) = 570$ pm, $n = 1.3636$, and $\varepsilon = 35.95$ were used in the following equation

$\Delta G^{*}_{\mathrm{OS}} = \frac{N_{\mathrm{A}}e^{2}}{16\pi\varepsilon_{0}}\left(\frac{1}{n^{2}} - \frac{1}{\varepsilon_{\mathrm{S}}}\right)\left(\frac{1}{2r_{A}} + \frac{1}{2r_{B}} - \frac{1}{\sigma_{AB}}\right)$

[c] $\Delta G^{*}_{\mathrm{IS}} = \Delta G^{*}_{11} - \Delta G_{\mathrm{Fuoss}} - \Delta G^{*}_{\mathrm{OS}}$

$$\Delta G^{*}_{\mathrm{Fuoss}} = -RT\ln K_{\mathrm{OS}},\ K_{\mathrm{OS}} = \frac{4\pi N_{\mathrm{A}}a^{3}}{3000}\exp\left(-\frac{U}{k_{\mathrm{B}}T}\right)\ \text{and}$$
$$U = \frac{z_{1}z_{2}e^{2}}{4\pi\varepsilon_{0}\varepsilon r k_{B}T(1 + Br\sqrt{\mu})} \tag{16}$$

where r's are the radii of the reactants, μ is the ionic strength and B is a parameter related to the Debye–Huckel theory for electrolyte solutions. By using these equations, the inner-sphere contribution to the activation Gibbs energy, $\Delta G^{*}_{\mathrm{IS}}$, for the self-exchange reaction of the $[Co(sep)]^{3+/2+}$ couple in acetonitrile was estimated as 39.1 kJ·mol^{-1} (a reported value of $k_{\mathrm{ex}} = 5.1$ kg·mol^{-1}·s^{-1} was used for this calculation [52]).

Table 4 lists the kinetic parameters calculated for the self-exchange reaction of the $[Zn(TPP)]^{+\cdot/*}$ couple in acetonitrile by applying the cross relation (Eq. 10) to the rate constant for the cross reaction of $[Zn(TPP)]^{*}$ with $[Co(sep)]^{3+}$ in acetonitrile observed in this study. Application of cross relation 12 yields $k_{\mathrm{ex}} = 4.9\times10^{9}$ kg·mol^{-1}·s^{-1} as the self-exchange rate constant for the $[Zn(TPP)]^{+\cdot/*}$ couple in acetonitrile when $Z^{2}_{12}/Z_{11}Z_{22} = 1$ was assumed: this value is consistent with that obtained by using Eq. 10 (8.39×10^{9} kg·mol^{-1}·s^{-1}), upon consideration of the accuracy inherent in these cross relations. Therefore, the assumption of $Z^{2}_{12}/Z_{11}Z_{22} = 1$ seems valid for the reactions even in acetonitrile and the analyses using Eqs. 10–16 are quite accurate: charges of the metal complexes such as $[Co(sep)]^{3+}$ and $[Co(sep)]^{2+}$ are effectively cancelled by the counter ions in acetonitrile, indicating that the same situation is also expected for the same reaction in ILs since the dielectric constants of the ILs used in this study are much smaller than that of acetonitrile ($\varepsilon = 37.5$ at 293 K, see also Appendix 1).

Equation 11 is expressed by Eq. 17 by using the corresponding activation Gibbs energies for each self-exchange reaction:

$$2\Delta G^{*}\left(\mathrm{Co}^{3+} + \mathrm{Zn(TPP)}^{*0}\right) = \Delta G^{*}_{\mathrm{OS}}(\mathrm{solv})_{\mathrm{Total}} + \left[\Delta G^{*}_{\mathrm{IS}}\left(\mathrm{Co}^{3+/2+}\right) + \Delta G^{*}_{\mathrm{IS}}\left(\mathrm{Zn(TPP)}^{+\cdot/*}\right)\right] + \Delta G^{0}\left(\mathrm{Co}^{3+} + \mathrm{Zn(TPP)}^{*0}\right) \tag{17}$$

where $\Delta G^{*}_{\mathrm{OS}}(\mathrm{solv})_{\mathrm{Total}} = \Delta G^{*}_{\mathrm{OS}}\left(\mathrm{Co}^{3+/2+}\right) + \Delta G^{*}_{\mathrm{OS}}\left(\mathrm{Zn(TPP)}^{+\cdot/*}\right)$. $\Delta G^{*}_{\mathrm{OS}}(\mathrm{solv})_{\mathrm{Total}}$ estimated by this equation, $\Delta G^{*}_{\mathrm{OS}}(\mathrm{solv\text{-}1})_{\mathrm{Total}}$, reflects the exact nature of the solvent ILs in the vicinity of the precursor and successor complexes. Estimated values of $\Delta G^{*}_{\mathrm{OS}}(\mathrm{solv\text{-}1})_{\mathrm{Total}}$ are listed in Table 5 for the reactions in BMIM, PMIM and HMIM: $\Delta G^{*}_{\mathrm{IS}}\left(\mathrm{Zn(TPP)}^{+\cdot/*}\right)$ and $\Delta G^{*}_{\mathrm{IS}}\left(\mathrm{Co}^{3+/2+}\right)$ in ILs were taken to be identical to those estimated for the self-exchange

Table 5 Estimated values of $\Delta G^*_{OS}(\text{solv-1})_{Total}$ and $\Delta G^*_{OS}(\text{solv-2})_{Total}$ for the reactions in BMIM, PMIM and HMIM

	k_{12} (kg·mol^{-1}·s^{-1})	ΔG^*_{12} (kJ·mol^{-1}[a])	ΔG^*_{OS}(Zn) (kJ·mol^{-1})	ΔG^0_{12} (kJ·mol^{-1})	$\Delta G^*_{OS}(\text{solv-1})_{Total}$ (kJ·mol^{-1})[b]	Pekar factor $1/n^2 - 1/\varepsilon$[c]	n[d]	ε_s[d]	$\Delta G^*_{OS}(\text{solv-2})_{Total}$ (kJ·mol^{-1})[e]	Pekar factor $1/n^2 - 1/\varepsilon_s$[f]
After correction for diffusion										
BMIM	3.65×10^7	4.07	0.844	−65.0	33.2	0.449	1.4267	13.7	30.9	0.418
PMIM	2.63×10^7	4.59	0.844	−65.3	34.6	0.468	1.4296	13.0	30.5	0.412
HMIM	2.01×10^7	5.08	0.844	−65.4	35.6	0.482	1.4302	12.7	30.3	0.410
Without correction for diffusion										
BMIM	3.06×10^7	4.51	1.59	−65.0	33.4	0.452	1.4267	13.7	30.9	0.418
PMIM	2.27×10^7	4.95	1.59	−65.3	34.5	0.467	1.4296	13.0	30.5	0.412
HMIM	1.78×10^7	5.38	1.59	−65.4	35.5	0.481	1.4302	12.7	30.3	0.410

[a] $\Delta G^*_{12} = -RT\ln\left(k_{12}/k_D\right)$

[b] $\Delta G^*_{IS}(\text{Co}) = 39.1\ \text{kJ}\cdot\text{mol}^{-1}$ for the calculation using the following equation: $2\Delta G^*_{12} = \Delta G_{OS}(\text{T}) + \Delta G^*_{IS}(\text{Zn}) + \Delta G^*_{IS}(\text{Co}) + \Delta G^0_{12}$

[c] Pekar factors of ILs estimated from $\Delta G^*_{OS}(\text{solv-1})_{Total}$

[d] Refractive indices and dielectric constants of bulk ILs

[e] Outer-sphere contributions ($\Delta G^*_{OS}(\text{solv-2})_{Total} = \Delta G^*_{OS}(\text{Zn})_{cal} + \Delta G^*_{OS}(\text{Co})_{cal}$ calculated using the following equation $\Delta G^*_{OS} = \frac{N_A e^2}{16\pi\varepsilon_0}\left(\frac{1}{n^2} - \frac{1}{\varepsilon_S}\right)\left(\frac{1}{2r_A} + \frac{1}{2r_B} - \frac{1}{\sigma_{AB}}\right)$, using $r(\text{Zn}) = 570$ pm and $r(\text{Co}) = 400$ pm, and the dielectric constants and refractive indices for bulk ILs

[f] Pekar factors for bulk ILs

reactions in acetonitrile since the inner-sphere contribution to the activation Gibbs energy is not dependent on the solvent [5].

Values of $\Delta G^*_{OS}(\text{solv})_{Total}$, $\Delta G^*_{OS}(\text{solv-2})_{Total}$, calculated using Eq. 15 are 30.9, 30.5 and 30.3 kJ·mol^{-1} (Table 5) in BMIM, PMIM and HMIM, when measured/reported refractive indices and dielectric constants for the bulk ILs are used in the calculations. The values of $\Delta G^*_{OS}(\text{solv-1})_{Total}$ and $\Delta G^*_{OS}(\text{solv-2})_{Total}$ in Table 4 seem close to each other, which indicates that the analyses employed in this study is reasonable. However, when we look into the details, the estimated $\Delta G^*_{OS}(\text{solv-1})_{Total}$ values increase in the order, BMIM < PMIM < HMIM, while theoretically calculated $\Delta G^*_{OS}(\text{solv-2})_{Total}$ increase in the opposite order, BMIM > PMIM > HMIM. Similar results were reported by Fawcett et al. for the adiabatic electron transfer process at the electrode for the Ferrocene/Ferricinium couple in ILs [61], indicating that the observation by Israelachvili and co-workers [28] together with the explanations by Nakamuta and Shikata [43] are valid even for the ILs in the vicinity of charged/polarized ions (see details in Appendix 2). It seems certain that the solvent macroscopic properties related to the Pekar factor, the refractive index and dielectric constant, are different from those for the bulk ILs in the vicinity of the charged encounter (precursor/successor) complexes: as discussed in the section of electrochemical studies and also indicated by the authors of references [28, 43, 61], ILs seem dissociated, or at least the distance between the cationic and anionic components are elongated, in the vicinity of the precursor/successor complexes for electron transfer reactions. As the component ions of ILs are positively and negatively charged, it is certain that the "dissociated" component ions of ILs exist as pairs, and probably changing partner ions in a concerted manner [1].

It is known that the refractive index is related to the polarizability α of a molecule by the Lorentz–Lorenz formula (Eq. 18).

$$\frac{n^2-1}{n^2+2} = \frac{N\alpha}{3\varepsilon_0} \tag{18}$$

where N is the number of molecules per unit volume. As the cationic and anionic components of dissociated ILs are expected to act as pairs even after dissociation (though they are not the tightly-bound pairs like bulk ILs), the polarizability and therefore the refractive index of such a pair may not be significantly different from those for the bulk ILs (polarizability is proportional to the volume of a molecule): it is expected that the polarizabilities for each cationic and anionic component of ILs are not largely different from those in the bulk ILs and therefore the *averaged* polarizability of dissociated ILs may not be very different from those of the bulk ILs.

By assuming that the refractive index is not affected by the dissociation of ILs, values of 23.6, 47.0 and 145 were calculated as the relative dielectric constants of BMIM, PMIM and HMIM, in the vicinity of a charged precursor/successor complex. Although such a large value as 145 may not be acceptable, this order of relative dielectric constants, BMIM < PMIM < HMIM, in the vicinity of the charged precursor/successor complexes explains the larger $\Delta G^*_{OS}(\text{solv-1})_{Total}$ observed for HMIM. However, this result also indicates that the refractive indices of the ILs around the charged species may also be slightly decreased from the values for bulk ILs in order to reproduce acceptable values for dielectric constants.

When a slow relaxation of solvent is involved in the activation process, the following solvent friction model may be invoked [61].

$$k = K_{OS}\kappa_{el}\tau_L^{-1}(\Delta G_{OS}^{*}/4\pi RT)^{\frac{1}{2}}\exp\left[-\frac{\Delta G_{OS}^{*}+\Delta G_{iS}^{*}}{RT}\right] \quad (19)$$

where τ_L is the longitudinal relaxation time of the solvent, defined by the product of the Debye relaxation time, τ_D, and (n^2/ε): $\tau_L = \left(\frac{n^2}{\varepsilon}\right)\tau_D = 3\,V_M\eta n^2/\varepsilon RT$. For viscous solvents with large molar volume V_M like ILs, τ_L may be longer compared with an ordinary molecular solvent. This relation accounts for the order of the observed rate constants for the cross reactions and $\Delta G_{OS}^{*}(\text{solv-1})_{Total}$: Grampp and co-workers discarded the possibility of this mechanism because the observed rate constants for their experiment did not exhibit the Pekar factor dependence [17]. However, as indicated by the results of this study, the electron self-exchange reactions in ILs may not exhibit the Pekar factor dependence since the solvent properties are altered around the precursor/successor complexes, by the dissociation of ILs. The expected decrease of τ_L was also confirmed by the experiments by Nakamura and Shikata [43] for the ILs in the vicinity of the electrode [see Appendix 2].

Dissociation of ILs is also expected around the polar transition state of the isomerization reaction of 4-dimethylamino-4′-nitro-azobenzene [1], and the intramolecular electron transfer/charge separation processes can be treated in the same way (Eq. 19). In the thermal isomerization reaction of 4-dimethylamino-4′-nitro-azobenzene, increased dielectric constant of ILs in the vicinity of the molecules stabilizes the polarized transition state and a smaller activation energy is expected for the reaction in HMIM than in BMIM ($E_a = 41.0$ kJ·mol^{-1} in HMIM and $E_a = 45.6$ kJ·mol^{-1} in BMIM). The observed smaller frequency factors for the reaction in HMIM (1.2×10^4 s^{-1} for HMIM and 1.4×10^6 s^{-1} for BMIM) may be attributed to the slower longitudinal relaxation times, τ_L, for HMIM than that of BMIM [43], although the activation energy and the frequency factor for the same reaction in PMIM ($E_a = 56.9$ kJ·mol^{-1} and 1.2×10^7 s^{-1}) cannot be explained by this model unless we assume some specific interaction between the solute and solvent molecules.

4 Conclusion

Results of the electrochemical measurements and the kinetic analyses, together with the observations by Israelachvili and co-workers [28], Nakamura and Shikata [43] and Fawcett et al. [62], indicate that ILs around charged metal complexes (including precursor/successor complexes for electron transfer reactions) dissociate and form local microstructures around the metal complexes [63]: dissociated anionic and cationic components of ILs seem to act as pairs even after dissociation and exchange the partner ions in a concerted manner [1, 43]. However, the thickness of such a modified solvent layer probably extends only to a couple of IL layers around the charged metal complexes (since the charges of the cobalt complex is only 3+), which is very much like the structure of the double layers at electrodes [28, 29].

The outer-sphere reorganization energies, $\Delta G_{OS}^{*}(\text{solv-1})_{Total}$, estimated from the experimental results are in the opposite order, BMIM < PMIM < HMIM to those calculated by using Marcus theory with bulk dielectric constants for ILs, $\Delta G_{OS}^{*}(\text{solv-2})_{Total}$, BMIM > PMIM > HMIM, which is attributed to the effect of the slightly decreased refractive index and increased dielectric constant of the medium caused by the induced dissociation of ionic liquids around charged metal/encountered complexes.

Dependence of the rate constants on the Pekar factor may not be observed when the dielectric constant and refractive index for the bulk IL are used for the calculation [17], since the dielectric constant and refractive index of the medium in the vicinity of the precursor/successor complexes are different from those for the bulk ILs.

It was shown that the methods employed in this study can be used to estimate the exact values of Pekar factors of ILs in the vicinity of polarized/charged precursor/successor complexes, although it may not be possible to evaluate the isolated values of the refractive indices and dielectric constants.

Previously reported activation energies and frequency factors for the isomerization reactions of 4-dimethylamino-4′-nitro-azobenzene in HMIM and BMIM [1] may be explained by the solvent friction model because of the decreased τ_L value as a result of the dissociation of ILs or elongation of the distance between the cationic and anionic components of ILs [43]. However, it was not possible to explain the kinetic parameters for the same reaction in PMIM.

Conventional approaches using a Born-type equation (dielectric continuum model) such as the Marcus theory) seems valid for the analyses of the reactions of relatively large metal complexes in ILs, while the analyses of the reactions of small organic molecules may not be successful [6] (see Appendix 2).

Acknowledgements We wish to thank JSPS KAKENHI Grant Numbers 16K05865 and 15K05451for financial support.

Appendix 1

Table 6 presents the Z_{ij} values calculated by assuming a couple of plausible dielectric constants ε_D for ILs as solvents (see text). It is obvious that the diffusion rate constant, Z_{AA}, is very small when cobalt complexes exist in solutions with formal charges. As the inner-sphere activation energy for the $[Co(sep)]^{3+/2+}$ couple is close to 40 kJ·mol^{-1}, the diffusion controlled rate constant has to be $>1\times10^8$ kg·mol^{-1}·s^{-1} to reproduce the exchange rate constant of ca. 5.1 kg·mol^{-1}·s^{-1}. However, the Z_{AA} values are still smaller than 10^7 kg·mol^{-1}·s^{-1}, even when the charges on the complexes are +1. Therefore, we may safely conclude that the assumption $Z_{AB}/Z_{AA}\ Z_{BB}=1$ is valid and the cobalt complexes are fully associated with the counter anions in ILs (at least the formal charges on either Co(III) or Co(II) complexes are completely cancelled). Note that the pair of a cation and an anion with the charge product of −3 is almost fully ion paired in solvents with $\varepsilon_D<30$ [23].

Appendix 2

Several previous articles offered new ideas concerning the modification of theoretical equations for dielectric properties of ILs on the basis of the non-linear response of solvents [64, 65]. Grampp and co-workers examined these new ideas by applying them to their experimental results for the self-exchange reaction of the $TCNE^{0/-}$ couple in various ILs, and clearly concluded that none of these theories reproduced their experimental observations [17].

We attempted to re-calculate the values of the Pekar factors for BMIM and HMIM using the experimental results reported by Grampp and co-workers: the outer-sphere activation Gibbs energy for the $TCNE^{0/-}$ self-exchange reaction was obtained by subtracting the

Table 6 Calculated Z_{ij} in $kg \cdot mol^{-1} \cdot s^{-1}$ by assuming various ionic charges for Co(III) and Zn(TPP) species in ILs and various relative dielectric constants estimated from the Born and MSA equations for different ILs

Charges	ε_D	$Z_{AB}/kg \cdot mol^{-1} \cdot s^{-1}$	$Z_{AA}/kg \cdot mol^{-1} \cdot s^{-1}$	$Z_{BB}/kg \cdot mol^{-1} \cdot s^{-1}$
$e = 2,3$				
BMIM	17.5	1.89×10^8	0.164	1.83×10^8
PMIM	17.5	1.68×10^8	0.146	1.62×10^8
HMIM	17.5	1.56×10^8	0.136	1.51×10^8
BMIM	13.7	1.89×10^8	2.69×10^{-4}	1.83×10^8
PMIM	13.0	1.68×10^8	4.83×10^{-5}	1.62×10^8
HMIM	12.7	1.56×10^8	2.14×10^{-5}	1.51×10^8
BMIM	24.3	1.89×10^8	98.1	1.83×10^8
PMIM	24.7	1.68×10^8	113	1.62×10^8
HMIM	24.9	1.56×10^8	120	1.51×10^8
BMIM	26.1	1.89×10^8	301	1.83×10^8
PMIM	26.6	1.68×10^8	354	1.62×10^8
HMIM	26.8	1.56×10^8	368	1.51×10^8
$e = 1,2$				
BMIM	17.5	1.89×10^8	4.90×10^5	1.83×10^8
PMIM	17.5	1.68×10^8	4.35×10^5	1.62×10^8
HMIM	17.5	1.56×10^8	4.04×10^5	1.51×10^8
BMIM	13.7	1.89×10^8	6.80×10^4	1.83×10^8
PMIM	13.0	1.68×10^8	3.67×10^4	1.62×10^8
HMIM	12.7	1.56×10^8	2.70×10^4	1.51×10^8
BMIM	24.3	1.89×10^8	3.32×10^6	1.83×10^8
PMIM	24.7	1.68×10^8	3.18×10^6	1.62×10^8
HMIM	24.9	1.56×10^8	3.07×10^6	1.51×10^8
BMIM	26.1	1.89×10^8	4.61×10^6	1.83×10^8
PMIM	26.6	1.68×10^8	4.44×10^6	1.62×10^8
HMIM	26.8	1.56×10^8	4.26×10^6	1.51×10^8
$e = 1,1$				
BMIM	17.5	1.89×10^8	1.36×10^7	1.83×10^8
PMIM	17.5	1.68×10^8	1.21×10^7	1.62×10^8
HMIM	17.5	1.56×10^8	1.13×10^7	1.51×10^8
BMIM	13.7	1.89×10^8	5.67×10^6	1.83×10^8
PMIM	13.0	1.68×10^8	4.02×10^6	1.62×10^8
HMIM	12.7	1.56×10^8	3.37×10^6	1.51×10^8
BMIM	24.3	1.89×10^8	3.13×10^7	1.83×10^8
PMIM	24.7	1.68×10^8	2.87×10^7	1.62×10^8
HMIM	24.9	1.56×10^8	2.71×10^7	1.51×10^8
BMIM	26.1	1.89×10^8	3.60×10^7	1.83×10^8
PMIM	26.6	1.68×10^8	3.31×10^7	1.62×10^8
HMIM	26.8	1.56×10^8	3.12×10^7	1.51×10^8

estimated inner-sphere activation energy (3.25 $kJ \cdot mol^{-1}$) from each total activation energy for the reported second-order rate constants observed in BMIM and HMIM. Grampp and co-workers used an experimentally estimated value of the geometry function, that

corresponds to ca. 510 pm for the radii of the TCNE and its anionic radical. As Eq. 15 and therefore the Pekar factor are very sensitive to the radii of reaction pairs, estimated Pekar factors were too large to be rationalized by any theories.

We found the experimentally obtained outer-sphere contribution to the activation Gibbs energies by Grampp and co-workers were reproduced when the radii of these species are 290–320 pm. Moreover, their experimental results are well reproduced when the Pekar factor for the reaction in HMIM is larger than that for the reaction in BMIM. This tendency is consistent with that observed in this study. Therefore, we conclude that modern theories [64, 65] cannot explain the experimental results reported by Grampp and co-workers nor the results obtained in this study. Note that our previous attempt to examine the contribution of the non-linear response of solvents to the outer-sphere electron transfer processes was not successful either, when self-exchange processes of metal complexes were examined in conventional molecular solvents [6].

We presume that the model proposed in this article, which is related to the modification of the solvent properties of ILs in the vicinity of charged precursor/successor complex because of the induced dissociation of ILs, is the most promising at this moment, at least when the classical/semi-classical treatment for the electron transfer reactions are employed [2–4].

In 2010 [43], Nakamura and Shikata investigated the dielectric constants of various ILs and found there are three regimes of dielectric relaxations, two of which are in the Debye regime: one corresponds to τ_2 in the following equation and was attributed to the rotational relaxation of *elongated* IL involving free rotation of the cationic component.

$$\varepsilon' = \frac{\varepsilon_1}{1+\overline{\omega}^2\tau_1^2} + \frac{\varepsilon_2}{1+\overline{\omega}^2\tau_2^2} + \frac{\varepsilon_3}{1+\overline{\omega}^2\tau_3^2} + \varepsilon_\infty$$

$$\varepsilon'' = \frac{\overline{\omega}\tau_1}{1+\overline{\omega}^2\tau_1^2} + \frac{\overline{\omega}\tau_2}{1+\overline{\omega}^2\tau_2^2} + \frac{(\overline{\omega}\tau_3)^{2-\alpha}}{1+\overline{\omega}^2\tau_3^2}$$

where ε' and ε'' are the in-phase and the out-of-phase components of dielectric responses, and at the limit of $\overline{\omega} = 0$, $\varepsilon_s = \varepsilon_1 + \varepsilon_2 + \varepsilon_3 + \varepsilon_\infty$ (α indicates the slowest response τ_3 is in the Cole–Cole regime). Nakamura and Shikata analyzed their results and concluded that (1) in the dissociated pair of ILs cationic components freely rotate and the distance between the cationic and anionic pair depended on the length of the substituents on the cationic component, (2) the dielectric constant of ILs increased with increasing the length of the substituents, and (3) the relaxation time was longer for the ILs with longer substituents on the cationic component for such dissociated pairs.

$$\frac{1}{\tau_{\mathrm{av}}} = \left(\frac{\varepsilon_1}{\varepsilon_1+\varepsilon_2+\varepsilon_3}\right)\frac{1}{\tau_1} + \left(\frac{\varepsilon_2}{\varepsilon_1+\varepsilon_2+\varepsilon_3}\right)\frac{1}{\tau_2} + \left(\frac{\varepsilon_2}{\varepsilon_1+\varepsilon_2+\varepsilon_3}\right)\frac{1}{\tau_3}$$

Although Nakamura and Shikata seem to believe the observed phenomena are related to the properties of the bulk ILs, it is clear that they observed properties of ILs in the vicinity of the electrodes (Israelachvili and co-workers [28] concluded that dissociation of ILs in the bulk is less than 0.1%).

In this study, we observed a similar increase of the dielectric constant in the vicinity of the transition state of *homogeneous* outer-sphere electron transfer reactions: the increase in the Pekar factor was in the order of the substituents on the imidazolium cation,

BMIM < PMIM < HMIM. In addition, we already reported similar dependence of the activation energy on the length of substituents for the *homogeneous first-order* thermal isomerization reactions of substituted azobenzene with polar transition state [1].

Therefore, it is certain that the distances between the cationic and anionic components of ILs elongate because of the dissociation of ILs in the vicinity of charged/polarized species (in *homogeneous* solutions), and the dielectric constant of the ILs in the vicinity of charged/polarized species increases with increasing length of the substituents on the imidazolium cation of the ILs.

References

1. Baba, K., Ono, H., Itoh, E., Itoh, S., Noda, K., Usui, T., Ishihara, K., Inamo, M., Takagi, H.D., Asano, T.: Kinetic study of thermal *Z* to *E* isomerization reactions of azobenzene and 4-dimethylamino-4′-nitroazobenzene in ionic liquids [1-R-3-methylimidazolium bis(trifluoromethylsulfonyl)imide with R = butyl, pentyl, and hexyl]. Chem. Eur. J. **12**, 5328–5333 (2006)
2. Sutin, N.: Theory of electron-transfer reactions—insights and hindsights. Progr. Inorg. Chem. **30**, 441–499 (1983)
3. Cannon, R.D.: Electron Transfer Reactions. Butterworth, London (1980)
4. Marcus, R.A.: On the theory of electron-transfer reactions. VI. Unified treatment for homogeneous and electrode reactions. J. Chem. Phys. **43**, 679–701 (1965)
5. Swaddle, T.W.: "Pressure-testing" Marcus-Hush theories of outer-sphere electron-transfer kinetics. Inorg. Chem. **29**, 5017–5025 (1990)
6. Takagi, H.D., Swaddle, T.W.: Estimation of the outer-sphere contribution to the activation volume for electron exchange reactions using the mean spherical approximation. Chem. Phys. Lett. **248**, 207–212 (1996)
7. Weaver, M.: Dynamical solvent effects on activated electron-transfer reactions: principles, pitfalls, and progress. Chem. Rev. **92**, 463–480 (1992)
8. Grampp, G., Jaenicke, W.: Kinetics of diabatic and adiabatic electron exchange in organic systems comparison of theory and experiment. Ber. Bunsenges. **95**, 904–927 (1991)
9. Rosokha, S.V., Newton, M.D., Head-Gordon, M., Kochi, J.K.: Mulliken-Hush elucidation of the encounter (precursor) complex in intermolecular electron transfer via self-exchange of tetracyanoethylene anion-radical. Chem. Phys. **324**, 117–128 (2006)
10. Fawcett, W.R., Opallo, M.: The kinetics of heterogeneous electron transfer reaction in polar solvents. Angew. Chem. **33**, 2131–2143 (1994)
11. Paul, A., Samanta, A.: Photoinduced electron transfer reaction in room temperature ionic liquids: a combined laser flash photolysis and fluorescence study. J. Phys. Chem. B **111**, 1957–1962 (2007)
12. Skrzypczak, A., Neta, P.: Diffusion-controlled electron-transfer reactions in ionic liquids. J. Phys. Chem. A **107**, 7800–7803 (2003)
13. Vieira, R.C., Falvey, D.E.: Photoinduced electron-transfer reactions in two room-temperature ionic liquids: 1-butyl-3-methylimidazolium hexafluorophosphate and 1-octyl-3-methylimidazolium hexafluorophosphate. J. Phys. Chem. B **111**, 5023–5029 (2007)
14. Bentley, C.L., Li, J., Bond, A.M., Zang, J.: Mass-transport and heterogeneous electron-transfer kinetics associated with the ferrocene/ferrocenium process in ionic liquids. J. Phys. Chem. C **120**, 16516–16525 (2016)
15. Fujita, K., Kuwahara, J., Nakamura, N., Ohno, H.: Communication—fast electron transfer reaction of azurin fixed on the modified electrode in hydrated ionic liquids. J. Electrochem. Soc. **163**, G79–G81 (2016)
16. Barrado, E., Rodriguez, J.A., Hernandez, P., Castrillejo, Y.: Electrochemical behavior of copper species in the 1-buthyl-3-methyl-imidazolium chloride (BMIMCl) ionic liquid on a Pt electrode. J. Electroanal. Chem. **768**, 89–101 (2016)
17. Mladenova, B.Y., Kattnig, D.R., Sudy, B., Chotoc, P., Grampp, G.: Are the current theories of electron transfer applicable to reactions in ionic liquids? An ESR-study on the TCNE/$TCNE^{-\cdot}$ couple. Phys. Chem. Chem. Phys. **18**, 14442–14448 (2016)
18. Belding, S.R., Rees, N.V., Aldous, L., Hardacre, C., Compton, R.G.: Behavior of the heterogeneous electron-transfer rate constants of arenes and substituted anthracenes in room-temperature ionic liquids. J. Phys. Chem. C **112**, 1650–1657 (2008)

19. Koch, M., Rosspeintner, A., Angulo, G., Vauthey, E.: Bimolecular photoinduced electron transfer in imidazolium-based room-temperature ionic liquids is not faster than in conventional solvents. J. Am. Chem. Soc. **134**, 3729–3736 (2012)
20. Liang, M., Kaintz, A., Baker, G.A., Marconcelli, M.: Bimolecular electron transfer in ionic liquids: are reaction rates anomalously high? J. Phys. Chem. B **116**, 1370–1384 (2012)
21. Creaser, I.I., Harrowfield, J.M., Herlt, A.J., Sargeson, A.M., Springborg, J., Geue, R.J., Snow, M.R.: Sepulchrate: a macrobicyclic nitrogen cage for metal ions. J. Am. Chem. Soc. **99**, 3181–3182 (1977)
22. Ratner, M.A., Levin, R.D.: A thermodynamic derivation of the cross-relations for rates of electron-transfer reactions. J. Am. Chem. Soc. **102**, 4898–4900 (1980)
23. Jordan, R.B.: Reaction Mechanisms of Inorganic and Organometallic Systems. Oxford University Press, Oxford (1998)
24. Yamada, A., Mabe, T., Yamane, R., Noda, K., Wasada, Y., Inamo, M., Ishihara, K., Suzuki, T., Takagi, H.D.: Flipping of the coordinated triazine moiety in Cu(I)–L2 and the small electronic factor, κel, for direct outer-sphere cross reactions: syntheses, crystal structures and redox behaviour of copper(II)/(I)–L2 complexes (L = 3-(2-pyridyl)-5,6-diphenyl-1,2,4-triazine). Dalton Trans. **44**, 13979–13990 (2015)
25. Bonhøte, P., Dias, A.-P., Papageorgiou, N., Kalyanasundaram, K., Gråtzel, M.: Hydrophobic, highly conductive ambient-temperature molten salts. Inorg. Chem. **35**, 1168–1178 (1996)
26. Dyson, P.J., Grossel, M.C., Srinivasan, N., Vine, T., Welton, T., Williams, D.J., White, A.J.P., Zigras, T.: Organometallic synthesis in ambient temperature chloroaluminate(III) ionic liquids. Ligand exchange reactions of ferrocene. J. Chem. Soc. Dalton Trans. **19**, 3465–3469 (1997)
27. Iijima, K.: Problems in analyzing metal complexes with fluorine. Technical Reports, Faculty of Science, Osaka University. **20**, 17–19 (2011)
28. Gabbie, M.A., Valtiner, M., Banquy, X., Fox, E.T., Henderson, W.A., Israelachvili, J.N.: Ionic liquids behave as dilute electrolyte solutions. Proc. Nat. Acad. Sci. USA **110**, 9674–9679 (2013)
29. Bard, A.J., Falkner, L.R.: Electrochemical Method. Wiley, New York (1980)
30. Seybold, P.G., Gouterman, M.: Porphyrins: XIII: Fluorescence spectra and quantum yields. J. Molec. Spectrosc. **31**, 1–13 (1969)
31. Gradyushko, A.T., Tsvirko, M.P.: Probabilities of inter-combination transitions in porphyrin and metalloporphyrin molecules. Opt. Spektrosc. **31**, 548–556 (1971)
32. Quimby, D.J., Longo, F.R.: Luminescence studies on several tetraarylporphins and their zinc derivatives. J. Am. Chem. Soc. **97**, 5111–5117 (1975)
33. Harriman, A.: Luminescence of porphyrins and metalloporphyrins. Part 1. Zinc(II), nickel(II) and manganese(II) porphyrins. J. Chem. Soc. Faraday. Trans. I **76**, 1978–1985 (1980)
34. Lukaszewicz, A., Karolczak, J., Kowalska, D., Maciejewski, A., Ziolek, M., Steer, R.P.: Photophysical processes in electronic states of zinc tetraphenyl porphyrin accessed on one- and two-photon excitation in the Soret region. Chem. Phys. **331**, 359–372 (2007)
35. Politis, T.G., Drickamer, H.G.: High pressure luminescence studies of metalloporphyrins in polymeric media. J. Chem. Phys. **74**, 263–272 (1981)
36. Wolynes, P.G.: Linearized microscopic theories of nonequilibrium solvation. J. Chem. Phys. **86**, 5133–5136 (1987)
37. Rips, I., Klafter, J., Jortner, J.: Dynamics of ionic solvation. J. Chem. Phys. **88**, 3246–3252 (1988)
38. McManis, G.E., Weaver, M.J.: Solvent dynamical effects in electron transfer: numerical predictions of molecularity effects using the mean spherical approximation. J. Chem. Phys. **90**, 1720–1729 (1989)
39. McManis, G.E., Gochev, A., Nielson, R.M., Weaver, M.J.: Solvent effects on intervalence electron-transfer energies for biferrocene cations: comparisons with molecular models of solvent reorganization. J. Phys. Chem. **93**, 7733–7739 (1989)
40. Faucett, W.R., Blum, L.: Estimation of the outer-sphere contribution to the activation parameters for homogeneous electron-transfer reactions using the mean spherical approximation. Chem. Phys. Lett. **187**, 173–179 (1991)
41. Matsumoto, M., Tarumi, T., Takahashi, I., Noda, T., Takagi, H.D.: Pressure dependence of the electrode potentials of some iron(III/II), cobalt(III/II), and Ni(III/II) couples in aqueous solution: Estimation of the reaction volumes for M(III)/M(II) couples. Z. Naturforch. **52b**, 1087–1093 (1997)
42. Daguenet, C., Dyson, P.J., Krossing, I., Oleinikova, A., Slattery, J., Wakai, C., Weinga, H.: Dielectric response of imidazolium-based room-temperature ionic liquids. J. Phys. Chem. B **110**, 12682–12688 (2006)
43. Nakamura, K., Shikata, T.: Systematic dielectric and NMR study of the ionic liquid 1-alkyl-3-methyl imidazolium. ChemPhysChem **11**, 285–294 (2010)
44. Rodriguez, J., Kirmaier, C., Holton, D.: Optical properties of metalloporphyrin excited states. J. Am. Chem. Soc. **111**, 6500–6506 (1989)

45. Fajer, J., Borg, D.C., Forman, A., Folton, R.H.: π-Cation radicals and dications of metalloporphyrins. J. Am. Chem. Soc. **92**, 3451–3459 (1970)
46. Sakuma, T., Ohta, T., Yagyu, T., Takagi, H.D., Inamo, M.: Copper(II)-assisted charge transfer quenching of the excited state of a zinc(II) porphyrin complex bearing a peripheral bipyridine moiety. Inorg. Chem. Commun. **38**, 108–111 (2013)
47. Aoki, K., Goshima, T., Kozuka, Y., Kawamori, Y., Ono, N., Hisaeda, Y., Takagi, H.D., Inamo, M.: Electron transfer reaction of porphyrin and porphycene complexes of Cu(II) and Zn(II) in acetonitrile. Dalton Trans. **0**, 119–125 (2009)
48. Luo, C., Guldi, D.M., Imahori, H., Tamaki, K., Sakata, Y.: Sequential energy and electron transfer in an artificial reaction center: formation of a long-lived charge-separated state. J. Am. Chem. Soc. **122**, 6535–6551 (2000)
49. Moore, J.W., Pearson, R.G.: Kinetics and Mechanism, 3rd edn, p. 290. Wiley, New York (1981)
50. Noyes, R.M.: Reaction Kinetics. In: Porter, G. (ed.) Progr. Pergamon Press, London (1961)
51. North, A.M.: The Collison Theory of Chemical Reactions in Liquids. Methuen, London (1964)
52. Doine, H., Swaddle, T.W.: Pressure effects on the self-exchange rates of cobalt(III/II) couples: evidence for adiabatic electron transfer in the bis(1,4,7-trithiacyclononane) and sepulchrate complexes. Inorg. Chem. **30**, 1858–1862 (1991)
53. Logan, S.R.: Effects of temperature on the rates of diffusion-controlled reactions. Trans. Faraday Soc. **63**, 1712–1719 (1967)
54. Weston, R.E., Schwarz, H.A.: Chemical Kinetics. Prentice-Hall, New Jersey (1972)
55. Sumi, H., Marcus, R.A.: Dynamical effects in electron transfer reactions. J. Chem. Phys. **84**, 4894–4914 (1986)
56. Sumi, H.: Theory on reaction rates in nonthermalized steady states during conformational fluctuations in viscous solvents. J. Phys. Chem. **95**, 3334–3350 (1991)
57. Hanggi, P., Borkovec, M.: Reaction-rate theory: 50 years after Kramers. Rev. Modern Phys. **62**, 251–341 (1990)
58. Kramers, H.A.: Brownian motion in a field of force and the diffusion model of chemical reactions. Physica **7**, 284–304 (1940)
59. Zahir, K., Espenson, J.H., Bakac, A.: Reactions of polypyridylchromium(II) ions with oxygen: determination of the self-exchange rate constant of oxygen $O_2/O_2O_2^-.O_2^-$. J. Am. Chem. Soc. **110**, 5059–5063 (1988)
60. Grace, M.R., Takagi, H.D., Swaddle, T.W.: A cross relation in volumes of activation for electron-transfer reactions. Inorg. Chem. **33**, 1915–1920 (1994)
61. Fawcett, W.R., Gaa´l, A., Misicak, D.: Estimation of the rate constant for electron transfer in room temperature ionic liquids. J. Electroanal. Chem. **660**, 230–233 (2011)
62. Grampp, G., Harrer, W., Jaenicke, W.: The role of solvent reorganization dynamics in homogeneous electron self-exchange reactions. J. Chem. Soc. Faraday Trans. I **1**(83), 161–166 (1987)
63. Hamaguchi, H., Ozawa, R.: Structure of ionic liquids and ionic liquid compounds: are ionic liquids genuine liquids in the conventional sense? Adv. Chem. Phys. **131**, 85–104 (2005)
64. Xiao, T., Song, X.: Reorganization energy of electron transfer processes in ionic fluids: a molecular Debye-Hückel approach. J. Chem. Phys. **138**, 114105–114112 (2013)
65. Kornyshev, A.A.: Non-local dielectric response of a polar solvent and Debye screening in ionic solution. J. Chem. Soc. Faraday Trans. II **79**, 651–661 (1983)